1

Truss Layout Optimization

This chapter presents the general problem of truss layout optimization. After a brief introduction to the standard theory of mathematical programming in section 1.1, section 1.2 derives the governing equations of truss structures. Then, section 1.3 states the basic problem of topology optimization. The equivalence between volume and compliance minimization problems is also studied by means of the necessary conditions of optimality. On this basis, section 1.4 progressively builds up a general formulation by adding different design settings. At each step, the numerical difficulties associated with these building blocks are explained. Finally, the optimization of nodal positions is considered in section 1.5, leading to the general design problem of truss geometry and topology optimization, which remains unsolved in the literature.

1.1. Standard theory of mathematical programming

Consider a general nonlinear optimization problem consisting of the minimization of an objective function subject to inequality and equality constraints [MOR 03]:

$$\min_{\mathbf{z} \in \mathbb{R}^{N_z}} \quad f(\mathbf{z}) \qquad [1.1a]$$

$$\text{subject to:} \quad g_i(\mathbf{z}) \leq 0, \ \forall i = 1, \ldots, N_g, \qquad [1.1b]$$

$$h_j(\mathbf{z}) = 0, \ \forall j = 1, \ldots, N_h, \qquad [1.1c]$$

where $f : \mathbb{R}^{N_z} \to \mathbb{R}$, $\mathbf{g} : \mathbb{R}^{N_z} \to \mathbb{R}^{N_g}$, $\mathbf{h} : \mathbb{R}^{N_z} \to \mathbb{R}^{N_h}$ are smooth functions and $\mathbf{z} \in \mathbb{R}^{N_z}$ is a vector of continuous variables. Smoothness of the objective function and the constraints is important to allow for a good prediction of the search direction by optimization algorithms. The feasible set of the optimization problem [1.1] is defined as:

$$Z := \left\{ \mathbf{z} \in \mathbb{R}^{N_z} \mid g_i\left(\mathbf{z}\right) \leq 0, \ h_j\left(\mathbf{z}\right) = 0, \ \forall i = 1, \ldots, N_g, \right.$$

$$\left. \forall j = 1, \ldots, N_h \right\}. \qquad [1.2]$$

In the feasible region, the inequality constraint $g_i\left(\mathbf{z}\right) \leq 0$ is said to be *active* if $g_i\left(\mathbf{z}\right) = 0$ and *inactive* if $g_i\left(\mathbf{z}\right) < 0$. To solve problem [1.1], we first transform it into an unconstrained optimization problem by introducing Lagrange multipliers $\boldsymbol{\lambda}_g \in \mathbb{R}_+^{N_g}$ and $\boldsymbol{\lambda}_h \in \mathbb{R}^{N_h}$ such that:

$$\mathcal{L}\left(\mathbf{z}, \boldsymbol{\lambda}_g, \boldsymbol{\lambda}_h\right) := f\left(\mathbf{z}\right) + \sum_{i=1}^{N_g} \lambda_{g,i} g_i\left(\mathbf{z}\right) + \sum_{j=1}^{N_h} \lambda_{h,j} h_j\left(\mathbf{z}\right). \qquad [1.3]$$

Thus, solving problem [1.1] amounts now to finding a stationary point to [1.3]. If $g_i\left(\mathbf{z}\right)$ is active, we ensure that the search direction points toward the feasible region by enforcing the dual feasibility $\lambda_{g,i} \geq 0$. If g_i is inactive, we can remove the constraint by setting the complementary slackness $\lambda_{g,i} g_i\left(\mathbf{z}\right) = 0$. These additional constraints are parts of the Karush–Kuhn–Tucker (KKT) optimality conditions [MOR 03]. Let $\mathbf{z}^*$ be a local minimizer of problem [1.1]. Provided that some regularity conditions hold, then there exists $\lambda_{g,i}$ and $\lambda_{h,j}$ such that the first-order necessary conditions of optimality, or KKT conditions, are satisfied:

$$\nabla f\left(\mathbf{z}^*\right) + \sum_{i=1}^{N_g} \lambda_{g,i} \nabla g_i\left(\mathbf{z}^*\right) + \sum_{j=1}^{N_h} \lambda_{h,j} \nabla h_j\left(\mathbf{z}^*\right) = 0, \qquad [1.4a]$$

$$h_j\left(\mathbf{z}^*\right) = 0, \ \forall j = 1, \ldots, N_h, \qquad [1.4b]$$

$$\lambda_{g,i} \geq 0, \ g_i\left(\mathbf{z}^*\right) \leq 0, \lambda_{g,i} g_i\left(\mathbf{z}^*\right) = 0, \ \forall i = 1, \ldots, N_g. \qquad [1.4c]$$

The *regularity conditions* or *constraint qualifications* of problem [1.1] are necessary conditions that enable a numerical treatment by standard algorithms of mathematical programming. There are many constraint qualifications in the literature (see [PET 73] for a comprehensive survey). Hereafter, the following three prominent conditions are listed:

– the *linear constraint qualification* implies that if g_i and h_j are affine functions, then all subsequent constraint qualifications are satisfied;

– the *linear-independence constraint qualification* holds if the gradients of active inequality constraints $\nabla g_i\left(\mathbf{z}^*\right)$ and equality constraints $\nabla h_j\left(\mathbf{z}^*\right)$ are linearly independent at $\mathbf{z}^*$;

– the *Mangasarian–Fromovitz constraint qualification* holds if the gradients of active inequality constraints $\nabla g_i\left(\mathbf{z}^*\right)$ and equality constraints $\nabla h_j\left(\mathbf{z}^*\right)$ are positive linearly independent at $\mathbf{z}^*$.

For the remainder, the special case of *linear programming* should be mentioned. Such an optimization problem minimizes a linear objective function subject to linear equality and inequality constraints with non-negative variables. The convexity of the problem implies that a local optimum is also a global optimum and authorizes an efficient treatment by optimization algorithms [ALE 01]. We will see in section 1.3 that, very often, it is possible to reformulate topology optimization problems so that linear programming applies.

1.2. Governing equations of truss structures

Before stating the structural optimization problem, let us start with some basic notations for a linear elastic truss structure as depicted in Figure 1.1. Using standard finite element concepts, we consider a pin-jointed structure

composed of N_n nodes interconnected by truss elements $e \in \{1, \ldots, N_b\}$. With $d \in \{2, 3\}$ being the spatial dimension and N_s being the number of support reactions, the number of degrees of freedom is $N_d = d.N_n - N_s$. The vector of nodal coordinates is denoted by $\mathbf{x} \in \mathbb{R}^{d.N_n}$, the vector of nodal displacements is denoted by $\mathbf{u} \in \mathbb{R}^{N_d}$ and the vector of external forces is denoted by $\mathbf{f} \in \mathbb{R}^{N_d}$ (excluding support reactions). The member force is $t_e \in \mathbb{R}$. The design parameters associated with every truss element are the length $l_e \in \mathbb{R}_+$ and the cross-sectional area $a_e \in \mathbb{R}_+$, which, together, give the member volume $v_e = a_e l_e \in \mathbb{R}_+$. Using these notations, the static equilibrium equations between the internal forces and the external loading are written into an expanded form as [PET 01]:

$$\sum_{e=1}^{N_b} t_e \boldsymbol{\gamma}_e = \mathbf{f}, \tag{1.5}$$

or more compactly

$$\mathbf{Bt} = \mathbf{f} \tag{1.6}$$

where, for all member $e = 1, \ldots, N_b$, $\boldsymbol{\gamma}_e \in \mathbb{R}^{N_d}$ represents the vector collecting the direction cosines, and $\mathbf{B} \in \mathbb{R}^{N_d \times N_b}$ is the so-called equilibrium matrix concatenating the vector of directions cosines, i.e. $\mathbf{B} = \begin{bmatrix} \boldsymbol{\gamma}_1 \ldots \boldsymbol{\gamma}_e \ldots \boldsymbol{\gamma}_{N_b} \end{bmatrix}$. Assuming small deformations, the linear compatibility condition between the nodal displacements $\mathbf{u} \in \mathbb{R}^{N_d}$ and the element elongation $\boldsymbol{\epsilon} \in \mathbb{R}^{N_b}$ is [PET 01]:

$$\boldsymbol{\gamma}_e^\top \mathbf{u} = \epsilon_e, \ \forall e = 1, \ldots, N_b, \tag{1.7}$$

or using the compact notation of the equilibrium matrix:

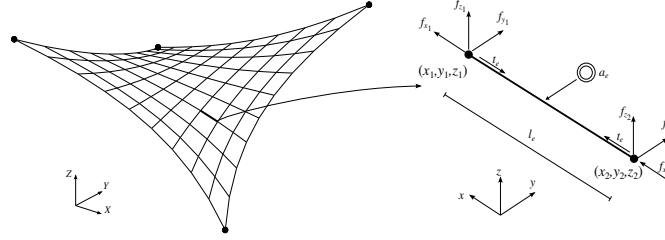$$\mathbf{B}^\top \mathbf{u} = \boldsymbol{\epsilon}. \tag{1.8}$$

Figure 1.1. *Notation for a truss element belonging, for instance, to a prestressed cable-net structure*

Then, for an elastic material of Young's modulus $E_e \in \mathbb{R}_+$, Hooke's law stating the relation between the axial stress $\sigma_e := t_e/a_e \in \mathbb{R}$ and strains $\varepsilon_e \in \mathbb{R}$ of the eth element is simply:

$$\frac{t_e}{a_e} = E_e \varepsilon_e, \ \forall e = 1, \ldots, N_b,$$
[1.9]

where the axial strain is given by the ratio of the elongation ϵ_e on the length, i.e.

$$\varepsilon_e = \frac{\epsilon_e}{l_e}, \ \forall e = 1, \ldots, N_b.$$
[1.10]

The solution to equations [1.5], [1.7] and [1.9] requires a thorough study of the statical and kinematical determinacies of the structural system. Pellegrino [PEL 86, PEL 93] identified four classes of truss structural assembly, as presented in Table 1.1. It is important to note that lightweight structures may belong to any of these classes. This will have serious consequences on the structural optimization process.

Frequently, the equilibrium equations for classical truss structures are formulated in terms of displacements by combining equations [1.5]–[1.9], leading to the following equality:

$$\mathbf{Ku} = \mathbf{f},$$
[1.11]

where, by definition of the reduced stiffness matrix,

$$\mathbf{K} := \sum_{e=1}^{N_b} \frac{E_e a_e}{l_e} \gamma_e \gamma_e^\top \in \mathbb{R}^{N_d \times N_d}. \qquad [1.12]$$

In the absence of mechanisms in the structural assembly (i.e. for assembly classes I and III), the stiffness matrix is symmetric positive definite and there exists a unique solution $\mathbf{u}$ to linear system [1.11]. In section 1.3, we will see that the treatment of equilibrium equations is a central issue in structural optimization and depends on whether the optimal structure might contain indeterminacy.

Class	Properties	Existence of solution	Example
I	$N_{ss} = 0$ $N_m = 0$	[1.5] has a unique solution for any loads. [1.7] has a unique solution for any elongations.	
II	$N_{ss} = 0$ $N_m > 0$	[1.5] has a unique solution for compatible loads. [1.7] has an infinity of solutions for any elongations.	
III	$N_{ss} > 0$ $N_m = 0$	[1.5] has an infinity of solutions for any loads. [1.7] has a unique solution for compatible elongations.	
IV	$N_{ss} > 0$ $N_m > 0$	[1.5] has an infinity of solutions for compatible loads. [1.7] has an infinity of solutions for compatible elongations.	

Table 1.1. *Classification of truss structural systems according to Pellegrino [PEL 93]. N_{ss} denotes the number of independent states of self-stress, or degree of hyperstaticity, and N_m denotes the number of independent zero-energy deformation modes, or mechanisms. The structure is said to be statically and kinematically determinate when $N_{ss} = 0$ and $N_m = 0$, respectively*

1.3. Layout and topology optimization

1.3.1. *Basic problem statement*

Layout optimization is among one of the most general approaches for structural design. Given a design domain subjected to boundary and loading conditions, layout optimization aims to find the best material distribution according to the problem definition. The stress-constrained minimum volume problem was first studied more than a century ago with the classical Michell's theorem [MIC 04], which gives the limit of economy for a structural frame. As discussed in section I.3, the scope is essentially theoretical but it provides essential information on how far a structure can be further optimized by relaxing constraints (in the general sense).

The exact optimal layout given by Michell's theory can be numerically approached via truss layout optimization. Based on a discretized model, the method follows the ground structure approach [DOR 64] where the design domain (Figure 1.2(a)) is divided into a grid of nodal points interconnected by tentative bars (Figure 1.2(b)). The most investigated strategy to solve the problem is topology optimization where both structural component sizes and system connectivity are simultaneously optimized. Cross-sectional areas $a \in \mathbb{R}^{N_b}$ are generally defined as continuous design variables. As such, topology optimization can be viewed as a sizing optimization problem with side constraints:

$$a_1, \ldots, a_e, \ldots, a_{N_b} \geq 0. \qquad\qquad [1.13]$$

The accuracy of truss topology optimization with respect to the exact analytical solution depends on the density of the grid, but also on the system connectivity: it can be limited to neighboring nodes (Figures. 1.2(c) and 1.2(d)), to a given

order of vicinity, or expanded to all nodes (Figures. 1.2(e) and 1.2(f)). Obviously, the latter case leads to better results, but at the expense of a considerable computational cost along with the presence of long and slender elements that are deemed inefficient to resist local buckling.
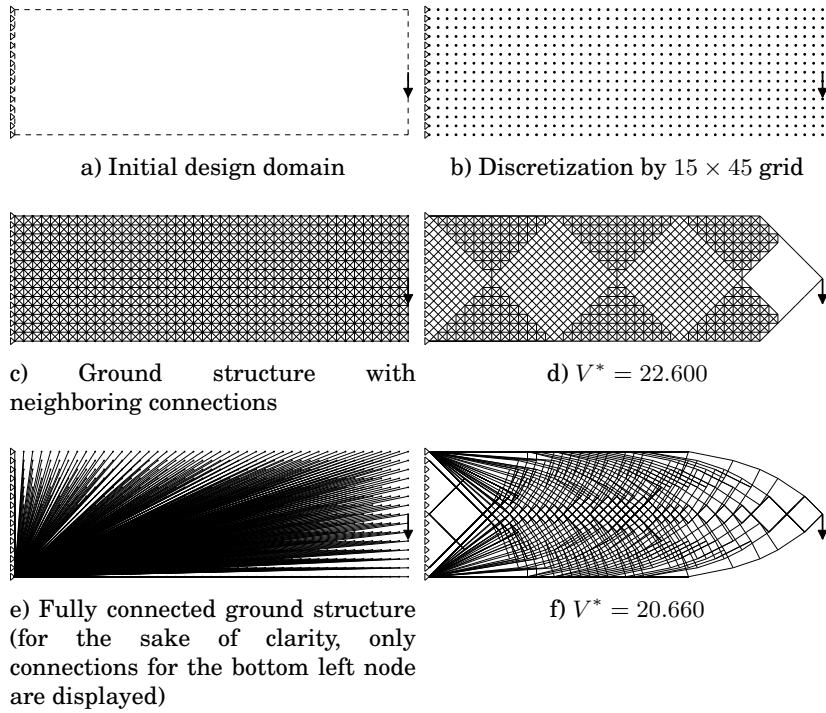
a) Initial design domain

b) Discretization by 15×45 grid

c)   Ground   structure   with neighboring connections

d) $V^* = 22.600$

e) Fully connected ground structure (for   the   sake   of   clarity,   only connections for the bottom left node are displayed)

f) $V^* = 20.660$

Figure 1.2. *A cantilever truss. The design domain is a rectangular panel of ratio 3:1. The supports are applied on leftmost nodes. A downward unit load is applied on the rightmost middle node. The exact analytical solution of 19.036 was calculated in [LEW 94]. The design domain and the initial ground structure are given in a) and b), respectively. For a ground structure with adjacently connected nodes c), the optimal layout is depicted in d). For a fully connected ground structure e), the optimal layout is depicted in f)*

Regarding   the   problem   definition,   most   of   the developments   in   the   literature   are   concentrated   on

compliance despite the fact that stress is among the most important consideration (see [BEN 03] for a comprehensive overview). Two main reasons explain this choice. First, compliance optimization problems are generally convex and thus easier to solve by mathematical programming [BEN 94]. Second, for single loading, compliance optimization is equivalent to the stress-constrained minimum volume problem [ACH 92] (see also section 1.3.2).

The goal of compliance optimization is to distribute a given amount of material to obtain a structure with maximum stiffness (i.e. of minimum compliance). Typically, the external work of applied loads is minimized subject to a global constraint on the allowable volume $\overline{V} \in \mathbb{R}_+$:

$$\min_{\mathbf{a} \in \mathbb{R}^{N_b}, \mathbf{u} \in \mathbb{R}^{N_d}} \mathbf{f}^T \mathbf{u} \qquad\qquad [1.14a]$$

$$\text{subject to: } \mathbf{K}\left(\mathbf{a}\right)\mathbf{u} = \mathbf{f}, \qquad\qquad [1.14b]$$

$$\sum_{e=1}^{N_b} v_e\left(\mathbf{a}\right) = \overline{V}, \ a_e \geq 0, \ \forall e = 1, \ldots, N_b. \quad [1.14c]$$

The enforcement of strict zero lower bounds on cross-sectional areas permits the removal of structural members. The resulting problem may converge to optimal structures with mechanisms: the system under unstable equilibrium is optimized for the applied loads but any perturbation of loads might lead to structural collapse. Stability issues are investigated in Chapter 2.

Equivalently, compliance optimization can be solved by minimizing the complementary (strain) energy. This switch is permitted because the total potential energy principle states

that the external work and the complementary energy are equal at equilibrium:

$$\mathbf{f}^\top \mathbf{u} = \sum_{e=1}^{N_b} \frac{t_e^2 l_e}{E_e a_e}. \qquad [1.15]$$

Using this objective function, the implementation benefits from the minimum complementary energy principle. In linear elasticity theory, among all stress components satisfying the static equilibrium equations, the actual stress distribution that enforces the compatibility condition is obtained by minimizing the complementary energy [KAN 05]. Hence, compatibility equations can be removed from the problem formulation and the problem is stated with static equilibrium equations [1.5]. Once again, a non negative lower-bound must be enforced to avoid infinite values of the complementary energy [1.15]. These considerations lead to the following problem [BEN 94]:

$$\min_{\mathbf{a}\in\mathbb{R}^{N_b}, \mathbf{t}\in\mathbb{R}^{N_b}} \sum_{e=1}^{N_b} \frac{t_e^2 l_e}{E_e a_e} \qquad [1.16a]$$

$$\text{subject to: } \sum_{e=1}^{N_b} t_e \boldsymbol{\gamma}_e = \mathbf{f}, \qquad [1.16b]$$

$$\sum_{e=1}^{N_b} v_e(\mathbf{a}) = \overline{V}, \; a_e \geq \overline{a}^{\,-}, \; \forall e = 1, \dots, N_b. \quad [1.16c]$$

Finally, we consider a tractable form of the classical problem that consists of reducing as much as possible the volume of material while enforcing that member stresses remain below the maximal allowable value $\overline{\sigma} \in \mathbb{R}_+$. Early work formulates this stress-constrained minimum volume problem in plastic design by neglecting the compatibility

condition [DOR 64, PED 70, HEM 73, ACH 96]:

$$\min_{\mathbf{a}\in\mathbb{R}^{N_b},\ \mathbf{t}\in\mathbb{R}^{N_b}} \sum_{e=1}^{N_b} a_e l_e \qquad\qquad [1.17a]$$

$$\text{subject to: } \sum_{e=1}^{N_b} t_e \boldsymbol{\gamma}_e = \mathbf{f}, \qquad\qquad [1.17b]$$

$$- a_e \overline{\sigma} \leq t_e \leq a_e \overline{\sigma},\ a_e \geq 0,\ \forall e = 1, \ldots, N_b, \quad [1.17c]$$

where stress constraints [1.17c] are multiplied by cross-sectional areas in order to avoid that $\sigma_e \to \pm\infty$ when $a_e \to 0$ for some vanishing members $e \in \{1, \ldots, N_b\}$ [BEN 94].

For solving problems [1.14], [1.16] and [1.17], it is important to observe that they are all equivalent in a certain sense. This property can be used to reformulate them as a linear programming problem, as presented in section 1.3.2.

1.3.2. *Problem equivalence and numerical solution*

This section shows that compliance and volume optimization under single loading lead to the same optimal truss and that a unique formulation in linear programming can be used for solving them. The study of optimality conditions is thus necessary for devising an efficient optimization process. For this, the relationship between compliance and volume optimization is first studied via the single-bar truss example shown in Figure 1.3.
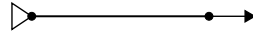

Figure 1.3. *The one-bar truss example. For convenience, the length is set at $l = 1$, the pulling force at $f = 1$, the Young's modulus at $E = 1$, the direction cosine at $\gamma = 1$, the allowable volume at $\overline{V} = 1$ and the limiting stresses at $\overline{\sigma} = 1$*

For compliance optimization, we intuitively understand that the process tends to increase a while enforcing the limit on the allowable volume of material $al = \overline{V}$, whereas volume optimization tends to decrease a while enforcing the limit on the allowable stress $\sigma < \overline{\sigma}$. It turns out that both problems converge to the same optimum in the design space (up to a factor that depends on the ratio between $\overline{V}$ and $\overline{\sigma}$). This can be demonstrated if there is a unique solution satisfying the KKT conditions for the following three formulations: the minimum compliance [1.14] identified by I, the minimum complementary energy [1.16] identified by II and the minimum volume [1.17] identified by III. For the single-bar truss, these problems are given by:

$$\min_{a^{\mathrm{I}} \in \mathbb{R}, u^{\mathrm{I}} \in \mathbb{R}} \left\{ f^{\mathrm{I}} u^{\mathrm{I}} \ \middle| \ \frac{E a^{\mathrm{I}}}{l} \gamma^2 u^{\mathrm{I}} = f^{\mathrm{I}}, \ a^{\mathrm{I}} l = \overline{V}, \ a^{\mathrm{I}} \geq 0 \right\}, \qquad [1.18]$$

$$\min_{a^{\mathrm{II}} \in \mathbb{R}, t^{\mathrm{II}} \in \mathbb{R}} \left\{ \frac{t^{\mathrm{II},2} l}{E a^{\mathrm{II}}} \ \middle| \ t^{\mathrm{II}} \gamma = f^{\mathrm{II}}, \ a^{\mathrm{II}} l = \overline{V}, \ a^{\mathrm{II}} \geq \overline{a}^{\,-} \right\}, \qquad [1.19]$$

$$\min_{a^{\mathrm{III}} \in \mathbb{R}, t^{\mathrm{III}} \in \mathbb{R}} \left\{ a^{\mathrm{III}} l \ \middle| \ t^{\mathrm{III}} \gamma = f^{\mathrm{III}}, \ -a^{\mathrm{III}} \overline{\sigma} \leq t^{\mathrm{III}} \leq a^{\mathrm{III}} \overline{\sigma}, \ a^{\mathrm{III}} \leq 0 \right\}. \qquad [1.20]$$

The Lagrangians of these problems are, respectively:

$$\mathcal{L}^{\mathrm{I}} = f^{\mathrm{I}} u^{\mathrm{I}} + \lambda_1^{\mathrm{I}} \left(\frac{E a^{\mathrm{I}}}{l} \gamma^2 u^{\mathrm{I}} - f^{\mathrm{I}} \right) + \lambda_2^{\mathrm{I}} \left(a^{\mathrm{I}} l - \overline{V} \right) + \lambda_3^{\mathrm{I}} \left(-a^{\mathrm{I}} \right), \qquad [1.21]$$

$$\mathcal{L}^{\mathrm{II}} = \frac{t^{\mathrm{II},2} l}{E a^{\mathrm{II}}} + \lambda_1 \left(t^{\mathrm{II}} \gamma - f^{\mathrm{II}} \right) + \lambda_2^{\mathrm{II}} \left(a^{\mathrm{II}} l - \overline{V} \right) + \lambda_3^{\mathrm{II}} \left(\overline{a}^{\,-} - a^{\mathrm{II}} \right), \qquad [1.22]$$

$$\begin{aligned} \mathcal{L}^{\mathrm{III}} = {} & a^{\mathrm{III}} l + \lambda_1^{\mathrm{III}} \left(t^{\mathrm{III}} \gamma - f^{\mathrm{III}} \right) + \lambda_2^{\mathrm{III}} \left(t^{\mathrm{III}} - a^{\mathrm{III}} \overline{\sigma} \right) \\ & + \lambda_3^{\mathrm{III}} \left(-t^{\mathrm{III}} - a^{\mathrm{III}} \overline{\sigma} \right) + \lambda_4^{\mathrm{III}} \left(-a^{\mathrm{III}} \right). \end{aligned} \qquad [1.23]$$

By differentiation, we obtain the KKT conditions for [1.21] by:

$$\lambda_1^{\mathrm{I}} \frac{E}{l} \gamma^2 u^{\mathrm{I}} + \lambda_2^{\mathrm{I}} l - \lambda_3^{\mathrm{I}} = 0, \ f^{\mathrm{I}} + \lambda_1^{\mathrm{I}} \frac{E a^{\mathrm{I}}}{l} \gamma^2 = 0, \qquad \text{[1.24a]}$$

$$\frac{E a^{\mathrm{I}}}{l} \gamma^2 u^{\mathrm{I}} = f^{\mathrm{I}}, \ a l^{\mathrm{I}} = \overline{V}, \ -a^{\mathrm{I}} \leq 0, \ \lambda_3^{\mathrm{I}} \geq 0, \ \lambda_3^{\mathrm{I}} a^{\mathrm{I}} = 0, \quad \text{[1.24b]}$$

for [1.22] by:

$$-\frac{t^{\mathrm{II},2} l}{E a^{\mathrm{II},2}} + \lambda_2^{\mathrm{II}} l - \lambda_3^{\mathrm{II}} = 0, \ \frac{2 t^{\mathrm{II}} l}{E a^{\mathrm{II}}} + \lambda_1^{\mathrm{II}} \gamma = 0, \qquad \text{[1.25a]}$$

$$t^{\mathrm{II}} \gamma = f^{\mathrm{II}}, \ a^{\mathrm{II}} l = \overline{V}, \ a^{\mathrm{II}} \geq \overline{a}^{\,-}, \ \lambda_3^{\mathrm{II}} \geq 0, \ \lambda_3^{\mathrm{II}} \left(\overline{a}^{\,-} - a^{\mathrm{II}} \right) = 0,$$
$$\text{[1.25b]}$$

and for [1.23] by:

$$l - \lambda_2^{\mathrm{III}} \overline{\sigma} - \lambda_3^{\mathrm{III}} \overline{\sigma} - \lambda_4^{\mathrm{III}} = 0, \ \lambda_1^{\mathrm{III}} \gamma + \lambda_2^{\mathrm{III}} - \lambda_3^{\mathrm{III}} = 0, \qquad \text{[1.26a]}$$

$$t^{\mathrm{III}} \gamma = f^{\mathrm{III}}, \ t^{\mathrm{III}} \leq a^{\mathrm{III}} \overline{\sigma}, \ -t^{\mathrm{III}} \leq a^{\mathrm{III}} \overline{\sigma}, \ -a^{\mathrm{III}} \leq 0, \qquad \text{[1.26b]}$$

$$\lambda_2^{\mathrm{III}}, \lambda_3^{\mathrm{III}}, \lambda_4^{\mathrm{III}} \geq 0, \qquad \text{[1.26c]}$$

$$\lambda_2^{\mathrm{III}} \left(t^{\mathrm{III}} - a^{\mathrm{III}} \overline{\sigma} \right) = 0, \ \lambda_3^{\mathrm{III}} \left(-t^{\mathrm{III}} - a^{\mathrm{III}} \overline{\sigma} \right) = 0, \ \lambda_4^{\mathrm{III}} a^{\mathrm{III}} = 0.$$
$$\text{[1.26d]}$$

For the same optimal design $a^{\mathrm{I}} = a^{\mathrm{II}} = a^{\mathrm{III}} = 1$ with state variables $u^{\mathrm{I}} = u^{\mathrm{II}} = u^{\mathrm{III}} = 1$, $t^{\mathrm{I}} = t^{\mathrm{II}} = t^{\mathrm{III}} = 1$ and $\sigma^{\mathrm{I}} = \sigma^{\mathrm{II}} = \sigma^{\mathrm{III}} = 1$, we can find Lagrange multipliers satisfying the optimality conditions [1.24]–[1.26]. We also verify that the compatibility condition [1.7] is satisfied at the optimum, i.e. $\sigma^* = (E/l) \gamma u^*$. Hence, the following assertions hold for the single loading case:

– the optimal compliance problems using the external work or complementary energy are identical;

– the compliance and volume optimization problems converge to an equivalent solution;

– this equivalent solution is a fully stressed design with the same strain energy density σ^2/E in each bar;

– such a solution obtained in plastic design automatically enforces the compatibility condition.

The assertions are still valid when the optimal structure is statically indeterminate [ACH 92] and for different yield stresses in tension and compression [ACH 96]. These properties allow us to reformulate the problem by linear programming algorithms.

To do so, the vector of internal forces can be expressed by non-negative tension force $\mathbf{t}^+ \in \mathbb{R}_+^{N_b}$ and compression force $\mathbf{t}^- \in \mathbb{R}_+^{N_b}$ such that $\mathbf{t} = \mathbf{t}^+ - \mathbf{t}^-$. The fully stressed design assumption allow us to define the cross-sectional area in terms of internal forces:

$$a_e\left(t_e^+, t_e^-\right) := \frac{1}{\sigma}\left(t_e^+ + t_e^-\right), \ \forall e = 1, \dots, N_b. \qquad [1.27]$$

Introducing these variable changes in the minimum volume problem results in the linear programming formulation:

$$\min_{\mathbf{t}^+ \in \mathbb{R}^{N_b}, \mathbf{t}^- \in \mathbb{R}^{N_b}} \ \sum_{e=1}^{N_b} \frac{l_e}{\sigma}\left(t_e^+ + t_e^-\right) \qquad [1.28a]$$

$$\text{subject to:} \ \sum_{e=1}^{N_b} \left(t_e^+ - t_e^-\right)\boldsymbol{\gamma}_e = \mathbf{f}, \qquad [1.28b]$$

$$t_e^+ \geq 0, t_e^- \geq 0, \ \forall e = 1, \dots, N_b. \qquad [1.28c]$$

The problem structure implies that either t_e^+ or t_e^- will be non-zero at the optimum. The use of the specific linear programming algorithm will efficiently find the global optimum for a very large design space [SOK 11].

Using this formulation, much effort is currently devoted to developing adding member procedures for high-density ground structures [GIL 03, SOK 11, SOK 13]. This loosely constrained problem in topology optimization with many nodes will converge to a continuous-like Michell's truss. However, the practical applicability is not obvious. For this reason, the formulation must be extended to consider more realistic designs.

1.4. Generalization

1.4.1. *Self-weight and multiple loading*

Truss topology optimization can be generalized in various ways to include additional design settings. A first aspect, often neglected in the literature, is self-weight of structural members and assemblies, which may have a considerable impact on the design of long-span lightweight structures. In this chapter, we assume that self-weight is equally carried by truss end-nodes while bending is neglected. Self-weight loads are considered as external forces that depend on the structural volume subject to gravity effects [BEN 03]. Let $\mathbf{g}_e \in \mathbb{R}^{N_d}$ be the vector of nodal gravitational forces for each member, the vector of external forces $\mathbf{f}$ becomes a design-dependent loading:

$$\mathbf{f} \xrightarrow{\text{self-weight}} \mathbf{f} + \sum_{e=1}^{N_b} v_e\left(\mathbf{a}\right) \mathbf{g}_e. \qquad [1.29]$$

This seemingly minor extension significantly influences the design problem as well as the numerical procedure. The external force vector is no longer constant but varies with respect to the design variables. This might lead to trivial situations where self-weight loads exactly balance the external loading, thus resulting in unstressed structures. In

the remainder, we will formally exclude such situations [BEN 03]:

$$\left\{ \mathbf{a} \in \mathbb{R}_+^{N_b} \ \middle| \ \sum_{e=1}^{N_b} v_e\left(\mathbf{a}\right) = \overline{V}, \ \mathbf{f} + \sum_{e=1}^{N_b} v_e\left(\mathbf{a}\right) \mathbf{g}_e = \mathbf{0} \right\} = \emptyset. \qquad [1.30]$$

Another important consideration is multiple loading [DA 97]. In practical applications, the structure is often subject to significant load changes. The designer must identify the framework of most critical loading cases for which the structure is designed accordingly. Let $\mathbf{f}_k \in \mathbb{R}^{N_d}$ be the vector of external forces, at each loading condition $k = 1, \ldots, N_c$ corresponds an equilibrium state. Hence, the system of equilibrium equations is expanded N_c times. In addition, the consideration of multiple loading conditions has consequences on the formulations and the design issues.

1.4.2. *Compliance optimization*

The extension of compliance optimization to include multiple loadings is not straightforward since there is one specific compliance measure by loading case:

$$c_k\left(\mathbf{a}, \mathbf{u}_k\right) = \left[\mathbf{f}_k + \sum_{e=1}^{N_b} v_e\left(\mathbf{a}\right) \mathbf{g}_e\right]^\top \mathbf{u}_k, \ \forall k = 1, \ldots, N_c. \quad [1.31]$$

Ideally, a structure simultaneously minimizing all specific compliances would be the optimal solution. However, such a solution does not exist in general, and a trade-off can be found by multicriteria optimization [MEL 12]. To combine these specific compliances in a single global measure, commonly accepted formulations are either the weighted-average or the worst-case compliance. In the former case, non-negative weights $w_k \in [0, 1]$ with $\sum_{k=1}^{N_c} w_k = 1$ are assigned to every specific compliance. Then, the weighted

sum of specific compliances is minimized subject to a global constraint on the allowable volume of material $\overline{V}$:

$$\min_{\substack{\mathbf{a} \,\in\, \mathbb{R}^{N_b} \\ \mathbf{u}_k \,\in\, \mathbb{R}^{N_d}}} \sum_{k=1}^{N_c} w_k c_k \left(\mathbf{a}, \mathbf{u}_k\right) \tag{1.32a}$$

$$\text{subject to: } \mathbf{K}\left(\mathbf{a}\right)\mathbf{u}_k = \mathbf{f}_k + \sum_{e=1}^{N_b} v_e\left(\mathbf{a}\right)\mathbf{g}_e, \ \forall k = 1,\dots,N_c \tag{1.32b}$$

$$\sum_{e=1}^{N_b} v_e\left(\mathbf{a}\right) = \overline{V}, \ a_e \geq 0, \ \forall e = 1,\dots,N_b. \tag{1.32c}$$

The latter case is a min-max optimization problem where the worst compliance over all loading cases is minimized:

$$\min_{\substack{\mathbf{a} \,\in\, \mathbb{R}^{N_b} \\ \mathbf{u}_k \,\in\, \mathbb{R}^{N_d}}} \ \max_{k=1,\dots,N_c} c_k\left(\mathbf{a}, \mathbf{u}_k\right) \tag{1.33a}$$

$$\text{subject to: } \mathbf{K}\left(\mathbf{a}\right)\mathbf{u}_k = \mathbf{f}_k + \sum_{e=1}^{N_b} v_e\left(\mathbf{a}\right)\mathbf{g}_e, \ \forall k = 1,\dots,N_c, \tag{1.33b}$$

$$\sum_{e=1}^{N_b} v_e\left(\mathbf{a}\right) = \overline{V}, \ a_e \geq 0, \ \forall e = 1,\dots,N_b. \tag{1.33c}$$

Problems [1.32] and [1.33] can be reformulated as convex problems and solved by several techniques, for instance semidefinite programming [KOČ 06] or second-order cone programming [MAK 10b].

1.4.3. *Volume optimization*

The most useful formulation to explore different design settings remains the minimum volume problem. There are

scenarios in which we wish to impose different stress constraints corresponding to different load cases, and possibly to different regions of the structure [LE 10]. For instance, stress constraints for permanent loads would be related to the material's yield limit whereas stress constraints for repetitive loads would be related to the material's endurance limit. In steel structures, stress constraints may also depend on the region of the structure when different steel strength classes or element types are used (strut, cable, etc.). Similarly, limiting stresses in tension and compression can be different. Other examples for displacements can be mentioned: tight displacement constraints can be enforced for permanent loads while accidental loadings are not restricted. Moreover, displacement constraints can be different following the directions. For all these reasons, stress and displacement bounds must have the possibility to take different values with respect to each loading case $k = 1, \ldots, N_c$, spatial direction $i = 1, \ldots, N_d$ and structural member $e = 1, \ldots, N_b$.

Unlike some particular cases (e.g. [MAK 10a]), the minimum volume problem with self-weight and multiple loading is generally not equivalent to compliance optimization [MEL 12]. Furthermore, the compatibility condition is required to obtain the actual stress field. To ensure meaningful solutions, limiting stresses in tension $\overline{\sigma}_{e,k}^{+} \in \mathbb{R}_+$ and compression $\overline{\sigma}_{e,k}^{-} \in \mathbb{R}_+$ are imposed for all structural loading cases and truss members. Moreover, nodal displacements can be restricted by different extrema denoted as $\overline{u}_{i,k}^{-} \in \mathbb{R}_+$ and $\overline{u}_{i,k}^{+} \in \mathbb{R}_+$. Finally, compressive members are also sized to remain below the Euler critical buckling load $\overline{\sigma}_{e}^{\mathrm{cr}}$. Setting $\mathbf{u}_k$ as the optimization variable, stresses are computed by combining compatibility equations [1.7] with Hooke's law [1.9] [KIR 89c] and the minimum volume problem subject to stress, local buckling [PED 93] and

displacement constraints [KOČ 97] takes the form [WAN 07]:

$$\min_{\substack{\mathbf{a} \,\in\, \mathbb{R}^{N_b} \\ \mathbf{u}_k \,\in\, \mathbb{R}^{N_d}}} \sum_{e=1}^{N_b} v_e\left(\mathbf{a}\right) \qquad\qquad\qquad \text{[1.34a]}$$

subject to: $\mathbf{K}\left(\mathbf{a}\right)\mathbf{u}_k = \mathbf{f}_k + \sum_{e=1}^{N_b} v_e\left(\mathbf{a}\right)\mathbf{g}_e,\ \forall k = 1,\dots,N_c,$

[1.34b]

$$-\overline{\sigma}_{e,k}^- \leq \frac{E_e}{l_e}\boldsymbol{\gamma}^\top \mathbf{u}_k \leq \overline{\sigma}_{e,k}^+,\ \forall e = 1,\dots,N_b,\ \forall k = 1,\dots,N_c,$$

[1.34c]

$$-\frac{E_e}{l_e}\boldsymbol{\gamma}_e^\top \mathbf{u}_k \leq \overline{\sigma}_e^{\mathbf{cr}}\left(\mathbf{a}\right),\ \forall e = 1,\dots,N_b,\ \forall k = 1,\dots,N_c,$$

[1.34d]

$$-\overline{u}_{i,k}^- \leq u_{i,k} \leq \overline{u}_{i,k}^+,\ \forall i = 1,\dots,N_d,\ \forall k = 1,\dots,N_c,$$

[1.34e]

$$a_e \geq 0,\ \forall e = 1,\dots,N_b. \qquad\qquad \text{[1.34f]}$$

Problem [1.34] is inherently non-convex and does not have a specific mathematical structure (e.g. linear or quadratic programming). A formulation of the form [1.34] is called *simultaneous analysis and design* in the literature [ARO 05]. In those formulations, both design and state variables are treated as optimization variables and the equilibrium equations set as equality constraints, which are solved by general-purpose nonlinear programming algorithms. Because we will follow the lines of this approach in our method, more details are given in Chapter 2.

Still, the most widespread approach to solving the stress-constrained optimization problem (especially for the design of continuum structures) is *nested analysis and design* [ARO 05]: displacement variables are removed from [1.14] by

performing a structural analysis via the displacement model [1.11]. However, truss topology optimization is an unusual structural optimization problem because the stiffness matrix may become singular when members vanish (see section 1.2). The intent of positive lower bounds $\overline{a}^{\,-} \in \mathbb{R}_+$ on cross-sectional areas is to ensure that the stiffness matrix remains non-singular. These lower bounds are assumed small enough to be structurally insignificant. The resulting problem is stated as:

$$\min_{\mathbf{a} \in \mathbb{R}^{N_b}} \sum_{e=1}^{N_b} v_e\left(\mathbf{a}\right) \qquad\qquad\qquad [1.35a]$$

subject to: $-\overline{\sigma}_{e,k}^{-} \leq \dfrac{E_e}{l_e} \boldsymbol{\gamma}^{\top} \mathbf{u}_k\left(\mathbf{a}\right) \leq \overline{\sigma}_{e,k}^{+},\ \forall e = 1, \dots, N_b,$

$$\forall k = 1, \dots, N_c, \qquad\qquad [1.35b]$$

$$-\frac{E_e}{l_e} \boldsymbol{\gamma}_e^{\top} \mathbf{u}_k\left(\mathbf{a}\right) \leq \overline{\sigma}_e^{\mathbf{cr}}\left(\mathbf{a}\right),\ \forall e = 1, \dots, N_b,$$

$$\forall k = 1, \dots, N_c, \qquad\qquad [1.35c]$$

$$-\overline{u}_{i,k}^{-} \leq u_{i,k}\left(\mathbf{a}\right) \leq \overline{u}_{i,k}^{+},$$

$$\forall i = 1, \dots, N_d,\ \forall k = 1, \dots, N_c, \qquad [1.35d]$$

$$a_e \geq \overline{a}^{\,-},\ \forall e = 1, \dots, N_b, \qquad\qquad [1.35e]$$

where the displacement variables are computed via a dedicated linear algebra routine:

$$\mathbf{u}_k\left(\mathbf{a}\right) = \mathbf{K}\left(\mathbf{a}\right)^{-1} \left(\mathbf{f}_k + \sum_{e=1}^{N_b} v_e\left(\mathbf{a}\right) \mathbf{g}_e \right),\ \forall k = 1, \dots, N_c. \qquad [1.36]$$

The solution process might converge to suboptimal solutions because some members are not completely eliminated from the ground structure [KIR 90a, CHE 92]. For more accuracy, Bruns [BRU 06] employs singular value decomposition but the analysis operation is more expensive.

However, both problems [1.34] and [1.35] are very difficult to solve because the numerical process is prone to numerical difficulties due to the presence of stress and local buckling constraints, as discussed in the following.

1.4.4. *Stress singularity*

Topology optimization with stress constraints is difficult to solve because the optimum might correspond to a singular point in the design space. This phenomenon is called *stress singularity* or *singular topology* in the literature. Sved and Ginos [SVE 68] first pointed out singular topologies. Hajela made the first representation of the corresponding feasible region [HAJ 82]. Kirsch also showed several properties of optimal topologies [KIR 87, KIR 89a].

For illustrative purposes, consider a variant of the three-bar truss example proposed by Kirsch [KIR 89b]. The structure and the design settings are depicted in Figure 1.4(a). To investigate various possibilities of optimal topologies, we introduce a non-negative parameter $\beta \in \mathbb{R}_+$ varying the cost of the second bar in the total volume function. Thus, the minimum volume problem subject to stress constraints is:

$$\min_{\mathbf{a} \in \mathbb{R}_+^3, \mathbf{u} \in \mathbb{R}^2} \left\{ a_1 l_1 + \beta a_2 l_2 + a_3 l_3 \;\middle|\; \mathbf{K}\left(\mathbf{a}\right) \mathbf{u} = \mathbf{f}, \right.$$

$$\left. -\overline{\sigma}_e^- \leq \frac{E_e}{l_e} \boldsymbol{\gamma}_e^\top \mathbf{u} \leq \overline{\sigma}_e^+, \; \forall e = 1, 2, 3 \right\}. \qquad [1.37]$$

Figure 1.4(b) depicts the corresponding design space. Using standard algorithms of mathematical programming, the solution process will converge to either point A or point B:

Point A: $a_1 = 0,$ $a_2 = 1,$ $a_3 = 0,$ if $\beta \leq 2,$ [1.38a]

Point B: $a_1 = 1,$ $a_2 = 0,$ $a_3 = 1,$ if $\beta \geq 2.$ [1.38b]
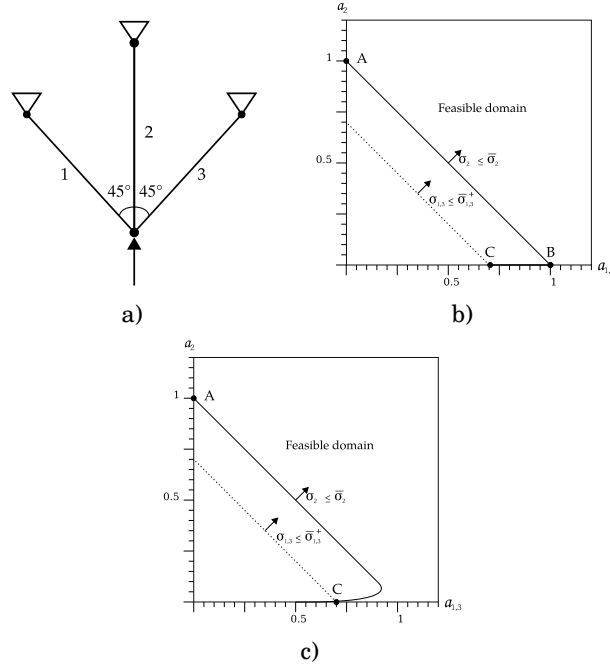
Figure 1.4. *The three-bar truss example with stress singularity. The representation of the initial ground structure is given in a). The system is subject to an upward unit load. Young's moduli are taken as $E_e = 1$, the length $l_e = 1$ and the limiting stresses are $\overline{\sigma}_e^- = 1$ and $\overline{\sigma}_e^+ = 1$ for all $e = 1, 2, 3$. The corresponding design space with respect to a_1 and $a_{2,3}$ for the case with singular optimum b) and using relaxed constraints c)*

The optimal volume of point B is $V^* = 2$. However, the true optimum for this problem is:

$$\text{Point A:} \quad a_1 = 0, \quad a_2 = 1, \quad a_3 = 0, \quad \text{if } \beta \leq \frac{1}{\sqrt{2}}, \quad [1.39a]$$

$$\text{Point C:} \quad a_1 = \frac{1}{\sqrt{2}}, \quad a_2 = 0, \quad a_3 = \frac{1}{\sqrt{2}}, \quad \text{if } \beta \geq \frac{1}{\sqrt{2}}. \quad [1.39b]$$

The value $V^* = \sqrt{2}$ of point C is below the optimal volume of point B. This demonstrates that optimization algorithms are unable to properly eliminate the redundant member 2. To figure this out, we expand the system $\mathbf{Ku} = \mathbf{f}$ into the

following two equilibrium and three compatibility equations:

$$\frac{\sqrt{2}}{2}a_1\sigma_1 - \frac{\sqrt{2}}{2}a_3\sigma_3 = 0, \qquad [1.40a]$$

$$-\frac{\sqrt{2}}{2}a_1\sigma_1 - a_2\sigma_2 - \frac{\sqrt{2}}{2}a_3\sigma_3 = 1, \qquad [1.40b]$$

$$\frac{\sqrt{2}}{2}u_x - \frac{\sqrt{2}}{2}u_y = \frac{\sigma_1}{E_1}l_1, \qquad [1.40c]$$

$$-u_y = \frac{\sigma_2}{E_2}l_2, \qquad [1.40d]$$

$$-\frac{\sqrt{2}}{2}u_x - \frac{\sqrt{2}}{2}u_y = \frac{\sigma_3}{E_3}l_3. \qquad [1.40e]$$

Stresses and displacements constitute the five unknowns of the linear system. We easily verify that solutions of equations [1.40] for points A and B also satisfy stress constraints. By contrast, at point C, the compatibility condition [1.40d] of member 2 enforces $\sigma_2 = -2/\sqrt{2}$. This value is inconsistent with stress constraints because the allowable stress $-\overline{\sigma}_2^- = -1$ is exceeded. Hence, both stress and compatibility constraints for member 2 cannot be satisfied simultaneously and point C is discarded by the optimization algorithm. The situation is paradoxical since member 2 does not exist at point C, but the optimization algorithm still handles those physically meaningless constraints.

Such a problem was recently identified as a *mathematical program with vanishing constraints* [ACH 08]. The major difficulty is that some regularity conditions of vanishing constraints – which are required to reach the true optimum – are violated. For instance, the dependence between the compatibility condition and stress constraint of member 2 violates the *linear-independence constraint qualification*, and thus all subsequent regularity conditions. Obviously,

assuming a plastic design (by neglecting compatibility equations) would prevent this conflict but the true optimum could be found only if the optimal topology is statically determinate [KIR 89b, KIR 89c, KIR 90a]. A general relaxation method was developed in the framework of mathematical programming [HOH 12, ACH 13].

Alternatively, the optimization problem can be stated in terms of cross-sectional areas by solving the equilibrium equations separately. Thus, the stress-constrained minimum volume takes the form:

$$\min_{\mathbf{a}\in\mathbb{R}^3_+} \left\{ a_1 l_1 + \beta a_2 l_2 + a_3 l_3 \ \Big| \ -\overline{\sigma}_e^- \leq \frac{E_e}{l_e}\boldsymbol{\gamma}_e^\top \left(\mathbf{K}\left(\mathbf{a}\right)^{-1}\mathbf{f}\right) \leq \overline{\sigma}_e^+, \right.$$

$$\left. \forall e = 1,2,3 \right\}. \qquad [1.41]$$

To avoid that $\sigma_e\left(\mathbf{a}\right) \to \pm\infty$ when $a_e \to 0$, some authors [HAJ 82, CHE 95] have proposed a variant but equivalent expression to make stress constraints feasible:

$$\left(\sigma_e\left(\mathbf{a}\right) - \overline{\sigma}_e^+\right) a_e \leq 0, \ \forall e = 1,\ldots,N_b, \qquad [1.42a]$$

$$\left(\overline{\sigma}_e^- - \sigma_e\left(\mathbf{a}\right)\right) a_e \leq 0, \ \forall e = 1,\ldots,N_b. \qquad [1.42b]$$

Despite the fact that the stress constraints of non-existing members seemingly vanish, the design space shown in Figure 1.4(b) shows that point C belongs to the strip BC. The difference of dimension between this degenerate subspace and the main feasible space is precisely the number of vanishing members. Standard algorithms of nonlinear programming cannot deal with these infinitesimally narrow strips. However, Cheng [CHE 95] pointed out that they are always connected to the main feasible design space.

This assertion has guided several authors to develop techniques to relax stress constraints by expanding the

region BC, as shown in Figure 1.4(c). Among others, Rozvany [ROZ 96] employed the Kreisselmeier–Steinhauser smooth framework function, but the most popular and widely studied technique for truss topology optimization remains the ϵ-relaxation method [CHE 97]. The basic idea is to introduce a relaxation parameter $\epsilon \geq 0$, which continuously decreases $\epsilon \rightarrow 0$ so that the original problem is recovered at the optimum [PET 01]. For this, parameter ϵ is introduced into the stress constraints as follows:

$$\left(\sigma_e \left(\mathbf{a} \right) - \overline{\sigma}_e^{\,+} \right) a_e \leq \epsilon, \ \forall e = 1, \ldots, N_b, \qquad [1.43a]$$

$$\left(\overline{\sigma}_e^{\,-} - \sigma_e \left(\mathbf{a} \right) \right) a_e \leq \epsilon, \ \forall e = 1, \ldots, N_b, \qquad [1.43b]$$

$$a_e \geq \epsilon^2, \ \forall e = 1, \ldots, N_b. \qquad [1.43c]$$

Nevertheless, Stolpe and Svanberg [STO 01] proved that the trajectory of the ϵ-relaxation method may be non-smooth and even discontinuous. Even worse, its application to moderate-size structures introduces additional local optima [STO 03].

1.4.5. *Local buckling singularity*

The consideration of local buckling constraints exhibits similar issues with stress constraints. The problem was first identified by Guo *et al*. [GUO 01]. To illustrate the problem, consider again the three-bar truss (Figure 1.5(a)). The minimum volume problem with local buckling constraints is:

$$\min_{\mathbf{a} \in \mathbb{R}_+^3, \mathbf{u} \in \mathbb{R}^2} \left\{ a_1 l_1 + \beta a_2 l_2 + a_3 l_3 \,\middle|\, \mathbf{K} \left(\mathbf{a} \right) \mathbf{u} = \mathbf{f}, -\frac{E_e}{l_e} \boldsymbol{\gamma}_e^\top \mathbf{u} \leq \overline{\sigma}_e^{\,\mathrm{cr}} \left(\mathbf{a} \right), \right.$$

$$\left. \forall e = 1, 2, 3 \right\}, \quad [1.44]$$

where $\overline{\sigma}_e^{\,\mathrm{cr}} \left(\mathbf{a} \right)$ represents the Euler critical buckling load written in terms of cross-sectional areas (see section 3.3 for

more details). Figure 1.5(b) depicts the corresponding design space. The true optimum is given by the following points:

$$\text{Point A:} \quad a_1 = 0, \qquad a_2 = 1, \quad a_3 = 0, \qquad \text{if } \beta \leq \frac{1}{\sqrt{2}}, \quad [1.45a]$$

$$\text{Point B:} \quad a_1 = \frac{1}{\sqrt{2}}, \quad a_2 = 0, \quad a_3 = \frac{1}{\sqrt{2}}, \quad \text{if } \beta \geq \frac{1}{\sqrt{2}}. \quad [1.45b]$$

The optimal volume is $V^* = 1$ at point A and $V^* = \sqrt{2}$ at point B. However, standard algorithms are unable to reach either point A or point B. The cause is the inconsistency between local buckling and compatibility constraints of vanishing members. On the one hand, we easily verify with equations [1.40] that compatibility equations enforce non-zero stresses. On the other hand, zero stresses are required to ensure the feasibility of local buckling constraints when $a_e \to 0$. Hence, both constraint types cannot be satisfied simultaneously.

As for stress constraints, the singularity also arises when the problem is stated in terms of cross-sectional areas only:

$$\min_{\mathbf{a} \in \mathbb{R}^3_+} \left\{ a_1 l_1 + \beta a_2 l_2 + a_3 l_3 \ \middle| \ -\frac{E_e}{l_e} \gamma_e^\top \left(\mathbf{K}\left(\mathbf{a}\right)^{-1} \mathbf{f} \right) \leq \overline{\sigma}_e^{\,\mathbf{cr}}\left(\mathbf{a}\right), \right.$$

$$\left. \forall e = 1, 2, 3 \right\}. \qquad [1.46]$$

The design space of Figure 1.5(b) shows that the optimal points belong to degenerate subspaces. Compared to stress constraints, the problem is even more critical because the feasible design domain is disjoint. Guo *et al.* [GUO 01] proposed a variant of the ϵ-relaxation method to reconnect the different parts by modifying the local buckling constraints as follows:

$$-\sigma_e\left(\mathbf{a}\right) - \overline{\sigma}_e^{\,\mathbf{cr}}\left(\mathbf{a}\right) \leq \epsilon, \ \forall e = 1, \ldots, N_b, \qquad [1.47]$$

The reconnected design space is depicted in Figure 1.5(c). Despite this modification, the feasible design domain is highly non-convex and the problem remains difficult to solve by optimization algorithms. Hence, the proposal was enhanced via a second-order smooth approximation of relaxed constraints. Applications are still limited to structures of moderate size.
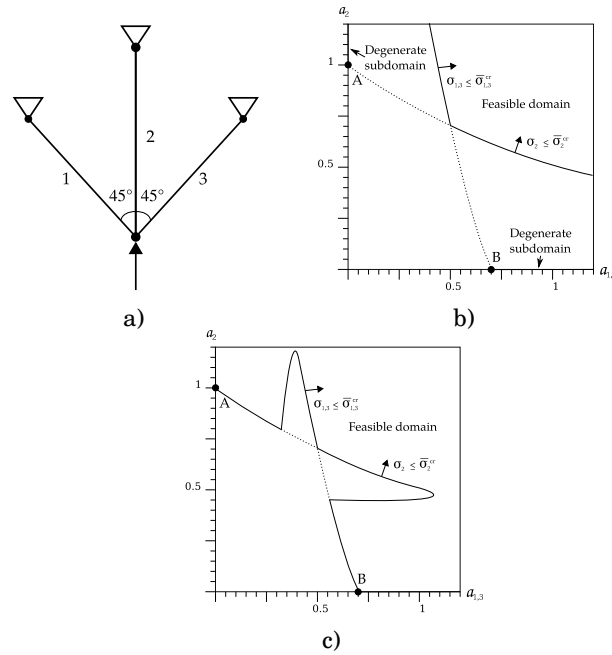

Figure 1.5. *The three-bar truss example with local buckling singularity. The representation of the ground structure is given in a). The system is subjected to a upward unit load. Young's moduli are taken as $E_e = 1$ and the length $l_e = 1$ for all $e = 1, 2, 3$. The design space is given in b) for the case with singular optimum and c) using relaxed constraints*

1.5. Truss geometry and topology optimization

1.5.1. *Optimization of nodal positions*

In the quest for more practical design methods, some recent works in topology optimization focused on

incorporating technological considerations to prevent short, thin and overlapping bars or to restrict the number of joints [GIL 05a, PRI 05]. Yet, truss layout optimization might also comprise the search for the optimal nodal locations; a natural way of dealing with these constraints. This feature is especially relevant in view of designing lightweight structures. In that case, the overall problem is called truss geometry and topology optimization. Kirsch [KIR 90b] pointed out that good results can be obtained with sparse ground structures by optimizing the structural geometry.

For this highly nonlinear problem, an important issue is how to define the geometrical variables. Computer-aided geometrical design parameterization [KEG 06] and sensitivity filtering techniques [BLE 09, LE 11] for freeform surfaces are unsuitable because they discard potentially interesting regions of the design space. On the contrary, the variable giving maximal control on the geometry is the position of nodes $\mathbf{x} \in \mathbb{R}^{d.N_n}$. This vector is defined on the set of permissible positions $X \subset \mathbb{R}^{d.N_d}$, which, in its general form, becomes:

$$X := \left\{ \mathbf{x} \in \mathbb{R}^{d.N_n} \mid g_i\left(\mathbf{x}\right) \leq \mathbf{0}, h_j\left(\mathbf{x}\right) = \mathbf{0},\ i = 1, \ldots, N_g, \right.$$

$$\left. j = 1, \ldots, N_h \right\}. \qquad [1.48]$$

The set X can be more or less difficult to enforce, depending on the vector functions of geometrical constraints $g_i\left(\mathbf{x}\right) \colon X \to \mathbb{R}^{N_g}$ and $h_j\left(\mathbf{x}\right) \colon X \to \mathbb{R}^{N_h}$. To mention a simple one, all nodes could lie within a bounding box apart from those coordinates where support conditions are prescribed:

$$X := \{\mathbf{x} \in \mathbb{R}^{d.N_n} \mid \overline{x}_i{}^- \leq x_i \leq \overline{x}_i{}^+,\ \forall i = 1, \ldots, N_d, \qquad [1.49\text{a}]$$

$$x_i = \overline{x}_i,\ \forall i = N_d + 1, \ldots, d.N_n\}. \qquad [1.49\text{b}]$$

Here, $\overline{x}_i{}^- \in \mathbb{R}$ and $\overline{x}_i{}^+ \in \mathbb{R}$ are, respectively, the lower and upper bounds of the ith nodal coordinate whereas $\overline{x}_i \in \mathbb{R}$ stands for the support reactions.

The impact of varying nodal coordinates has consequences on the member length l_e and the vector of direction cosines γ_e. For these functions, the following formula holds (see [ACH 07] for the proof):

$$l_e : X \to \mathbb{R}_+, \ \mathbf{x} \mapsto l_e\left(\mathbf{x}\right) := \frac{1}{\sqrt{2}} \|\mathbf{C}_e \mathbf{x}\|_2, \ \forall e = 1, \dots, N_b, \quad [1.50]$$

$$l_e^2 : X \to \mathbb{R}_+, \ \mathbf{x} \mapsto l_e^2\left(\mathbf{x}\right) := \mathbf{x}^\top \mathbf{C}_e \mathbf{x}, \ \forall e = 1, \dots, N_b, \quad [1.51]$$

$$\boldsymbol{\gamma}_e : \mathcal{X} \to \mathbb{R}^{N_d}, \mathbf{x} \mapsto \boldsymbol{\gamma}_e\left(\mathbf{x}\right) := \frac{1}{l_e\left(\mathbf{x}\right)} \mathbf{P}\mathbf{C}_e \mathbf{x}, \ \forall e = 1, \dots, N_b,$$
$$[1.52]$$

where $\|.\|_2$ denotes the Euclidean norm, $\mathbf{C}_e \in \mathbb{R}^{d.N_n \times d.N_n}$ is a symmetric, positive semidefinite assembly matrix containing exactly d^3 non-zero entries of ± 1 and $\mathbf{P} \in \mathbb{R}^{N_d \times d.N_n}$ relates the system in non-reduced coordinates to the system in reduced coordinates. Note that l_e and $\boldsymbol{\gamma}_e$ are present almost everywhere in volume and compliance problem formulations. In particular, the global stiffness matrix in reduced coordinates can be formally defined as the following matrix-valued function with respect to the design variables:

$$\mathbf{K} : \mathbb{R}_+^{N_b} \times X \to \mathbb{R}^{N_d \times N_d}, \ (\mathbf{a}, \mathbf{x}) \mapsto \mathbf{K}\left(\mathbf{a}, \mathbf{x}\right)$$

$$:= \sum_{e=1}^{N_b} \frac{E_e a_e}{l_e\left(\mathbf{x}\right)} \boldsymbol{\gamma}_e\left(\mathbf{x}\right) \boldsymbol{\gamma}_e^\top\left(\mathbf{x}\right). \quad [1.53]$$

Besides the nonlinear behavior, the variation of nodal positions poses some numerical difficulties when dealing with mathematical programming. This issue is discussed in section 1.5.2.

1.5.2. *Melting node effect*

In optimal geometries, the *melting node effect* refers to members vanishing due to the melting of truss end nodes. The phenomenon was first identified by Achtziger [ACH 06]. To give an illustrative example, consider the five-bar truss depicted in Figure 1.6(a). For this example, the position of nodes 2 and 3 are optimized along the vertical direction without restriction. With the design variables $(\mathbf{a}, \mathbf{x})$, the minimum volume problem subject to stress constraints is:

$$
\min_{\substack{\mathbf{a} \in \mathbb{R}^5_+ \\ \mathbf{u} \in \mathbb{R}^4 \\ \mathbf{x} \in X}} \left\{ \sum_{e=1}^{5} a_e l_e(\mathbf{x}) \,\middle|\, \mathbf{K}(\mathbf{a}, \mathbf{x})\,\mathbf{u} = \mathbf{f}, -\overline{\sigma}_e^- \leq \frac{E_e}{l_e(\mathbf{x})} \gamma_e(\mathbf{x})\,\mathbf{u} \leq \overline{\sigma}_e^+, \right.
$$

$$
\left. \forall e = 1, \ldots, 5 \right\}. \tag{1.54}
$$

The true optimum of $V^* = 2.5$ includes melting nodes 2 and 3 (Figure 1.6(c)). However, standard algorithms of mathematical programming are unable to reach the solution because the presence of melting nodes causes serious convergence difficulties: the solution process will move close to the optimum (Figure 1.6(b)) without being able to find a KKT point. At the vicinity of the solution, the algorithm suddenly exhibits an erratic behavior with zigzags between two non-optimal points.

The length function is the bottleneck for the admission of melting nodes in optimal structures. At melting nodes, the length vanishes, i.e. $\|\mathbf{C}_e \mathbf{x}\|_2 = 0$ for some $e \in \{1, \ldots, N_b\}$. The consequence for the solution process is twofold. First,

consider the derivative of the length function [1.50] with respect to the nodal coordinates:

$$\nabla l_e \left(\mathbf{x} \right) = \frac{\mathbf{C}_e \mathbf{x}}{\| \mathbf{C}_e \mathbf{x} \|_2}, \ \forall e = 1, \ldots, N_b. \qquad [1.55]$$

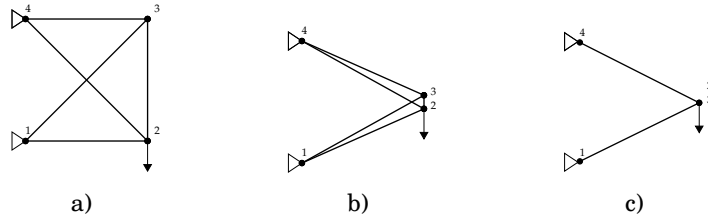a)   b)   c)

Figure 1.6. *The three-bar truss example. The representation of the initial ground structure is based on a square of unit side and given in a). A downward unit load is applied on node 2. Young's moduli are taken as $E_e = 1$ and limiting stresses are $\overline{\sigma}_e^- = 1$ and $\overline{\sigma}_e^+ = 1$ for all $e = 1, \ldots, 5$. The solution close to the optimum is given in b) and the actual optimum in c)*

A close inspection reveals that the derivative is undefined for melting nodes since the length appears in the denominator. This prevents the determination of a KKT point.

Second, the optimization problem involves some functions (e.g. the stiffness [1.53] and the direction cosine [1.52]), which are undefined for melting nodes since, once again, the length appears in the denominator. A common approach to avoid this is to define the set of permissible positions X_0 so that the melting node effect cannot occur [XIA 13]:

$$X_0 := \left\{ \mathbf{x} \in X \mid l_e \left(\mathbf{x} \right) \neq 0, \ \forall e = 1, \ldots, N_b \right\}. \qquad [1.56]$$

However, this approach is cumbersome and possibly intractable for complex applications. Actually, optimal geometries with melting nodes are even desirable to the extent that such solutions may achieve more effective results [BEN 93, BEN 94, RAH 08].

1.6. Concluding remarks

In this chapter, we have described truss layout optimization in a mathematical programming context. First, topology optimization for minimum volume and compliance problems under single loading was stated along with the equivalence between both problems. Then, the formulation was progressively extended to obtain the general problem of truss geometry and topology optimization including member self-weight and multiple loading, as well as stress, displacement and local buckling constraints. For these extensions, the singularities that arise in optimum solutions were identified.

In the literature, truss geometry and topology optimization remain unsolved. Thus, the purpose of Chapter 1 is to develop a novel formulation to treat the problem by mathematical programming.